Computational design of molecularly imprinted polymer for direct detection of melamine in milk

Ferdia Bates[1], Mirko Busato[2], Elena Piletska[3], Michael J. Whitcombe[3], Kal Karim[3], Antonio Guerreiro[3], Alejandro Giorgetti[2], Sergey Piletsky[3], Manel del Valle[1*]

1. Sensors & Biosensors Group, Department of Chemistry, Universitat Autònoma de Barcelona, 08193 Bellaterra, Spain

2. Department of Biotechnology, University of Verona, Strada le Grazie 15, 37134 Verona, Italy

3. Chemical Biology, Department of Chemistry, University of Leicester, Leicester LE1 7RH, UK

***** Corresponding Author: **manel.delvalle@uab.es**

Abstract

A novel protocol for use of molecularly imprinted polymer (MIP) in analysis of melamine is presented. Design of polymer for melamine has been achieved using a combination of computational techniques and laboratory trials, the former greatly reducing the duration of the latter. The compatibility and concerted effect of monomers and solvents were also investigated and discussed. Two novel open source tools were presented which are: the online polymer calculator from mipdatabase.com and the application of the Gromacs modelling suite to determine the ideal stoichiometric ratio between template and functional monomer. The MIP binding was characterised for several structural analogues at 1-100 μM concentrations. The use of DVB as cross-linking polymer and itaconic acid as functional monomer allowed synthesis of MIP with imprint factor for melamine IF=2.25. This polymer was used in HPLC for the rapid detection of melamine in spiked milk samples with an experimental run taking 7-8 minutes. This approach demonstrated the power of virtual tools in accelerated design of MIPs for practical applications.

Keywords: melamine, milk, molecularly imprinted polymer, molecular modelling, molecular dynamics

1. Introduction

Molecularly imprinted polymers (MIPs) have become a widely known and growing part of the field of polymer chemistry (1,2). Their great advantage is that they can be used in a wide range of environments and applications due to their high thermal and chemical stability. Additionally, high specificity and affinity in MIPs can be achieved by tailoring of their binding site at a molecular level. Although there are several formats of imprinting protocols available, by far the most popular method used in practice remains bulk imprinting, where solution containing template and monomers is polymerised to form a solid 'brick' which can then be broken, washed and used as the specific application requires such as the packing media of high performance liquid chromatography (HPLC) or solid phase extraction (SPE) columns or as the detection element of molecular sensors (2). Though it is the most tried and tested technique with a minimal number of interdependent steps, a notable challenge of the traditional molecular imprinting strategy of bulk imprinting can be seen when the molecular template selected has a low solubility in organic solvents. The solubility of the template can be increased by the addition of an appropriate functional monomer (FM), as is done in this present study to great effect; however the phase separation during polymerisation still can lead to the precipitation of the template back into the solution. This danger of template precipitation can be further minimised by the use of a co-monomer with a higher affinity to the template, however this can reduce the specificity of the polymer. Indeed, the solubility of the template in the porogen and the manner in which it interacts with the functional monomers can markedly affect the efficiency of the imprinting process (3).

Melamine, a highly nitrogenous compound, is a heterocyclic triazine. It is used extensively in the synthesis of melamine formaldehyde resin which is, in turn, used in the fabrication of everyday products such as laminates, fabric coatings, commercial filters, glues and adhesives in addition to its general use in food containers and various common kitchenwares (4). Given its close proximity to food stuffs, the need to accurately detect and monitor it is paramount, especially when melamine combines with cyanuric acid (5–7). The hydrogen bonded complex of the two molecules is highly insoluble and precipitates in the kidneys to form stones which can lead to potentially fatal kidney failure (8).

Due to the aforementioned nitrogen content, counting for two thirds of its molecular mass, adulteration of dairy products with melamine has been employed as a method of artificially augmenting the apparent crude protein content (9) and as a cheap food supplement in cattle feed (10). Contamination of infant formula and pet food with melamine has caused a global scandal following the deaths of a number of babies and the hospitalisation of several thousand more (11). n 2004 the World Health Organisation (WHO) established a tolerable daily intake (TDI) of melamine of 0.2 mg/kg of body mass, a reduction from the previous level of 0.63 mg/kg set by the American food and drug administration (FDA) based on data collected in 1983 (4).

As a result the call was issued for more discriminating detection methods for melamine. For this reason, great efforts have been made in recent years to develop reliable methods for the detection for this molecule. Exhaustive research has been performed on the application of aptamers, immunoassays, colorimetric and electrochemical sensors for analysis of melamine (4,12). Unfortunately these approaches suffer from high price and limited dynamic and thermal stability of specific binders used in the assays and sensors. It is logical then that the application of MIPs for the detection of melamine has been attempted using several different imprinting and polymerisation methods.

The study herein details the design and development process of a melamine imprinted polymer utilising itaconic acid (IA) and divinylbenzene (DVB) as the functional monomer and cross-linker respectively. These components, along with the porogenic solvent, dimethyl sulfoxide (DMSO) were selected with the aid of a computational algorithm to rank monomers affinity toward melamine; the affinity rankings were confirmed with complimentary laboratory trials. Additionally, ideal stoichiometric ratios between melamine and IA were calculated using two independent protocols the second of which, utilising the open source modelling suite, Gromacs (13), has not been applied to this task prior to current work. The polymerisation method and temperature were optimised to produce a polymer most suitable for use as packing media for a HPLC column. HPLC mobile phase composition and isocratic flow rate was also optimised for separation efficiency, measurement time and resolution. The MIP was characterised for selectivity and specificity against several structural analogues before being used for the detection of melamine in liquid and powdered milk samples. Rapid and selective detection of melamine was achieved with the optimised process taking 7-8 minutes. The maximum imprint factor of the polymer column was calculated to be IF=2.25 and this showed discriminative preference for melamine at concentrations from 1 to 100 μM.

2. Experimental

2.1 Reagents

Melamine, acetoguanamine, cyanuric acid, urea, triazine, itaconic acid (IA), divinylbenzene (80% mixture of isomers) (DVB), dimethyl sulfoxide (DMSO), 1,1' azobis-cyclohexanecarbonitrile (AICN), 2,2′-azobis 2-methylpropionitrile (AIBN) and formic acid were all purchased from Sigma-Aldrich, UK. All reagents and solvents were analytical or HPLC grade and were used without any additional purification except for DVB which was technical grade. All water used was triple

distilled and deionised to a resistivity of 18.2 MΩ·m^{-1} by a Milli-Q purification system (Millipore, Billerica, MA, USA). Real milk samples were purchased at random at local supermarkets in Leicester, UK.

2.3 Molecular modelling

2.3.1 Virtual screening of molecules

The molecular modelling protocol employed to determine and rank candidate monomer molecules for effective binding with the template has been extensively documented elsewhere (14,15). This method uses the DREAM method of the LEAPFROG algorithm, a component of SYBYL (v. 7.3) modelling suite (Tripos Inc., St. Louis, MO, USA). The parameters of the binding upon which the binding score is calculated, have been optimised to favour the ability of monomers to form strong molecular complex with the template. All libraries screened consisted of molecular structures minimised to an energy of 0.01 kcal·mol^{-1}.

Three libraries were compiled to be used in the MIP design process. A range of acidic, basic and neutral FMs were modelled with additional charged structures where appropriate. These were acrylamido-2-methyl-1-propanesulfonic acid (AMPSA), acrylic acid (AA), IA, methacrylic acid (MAA), trifluoromethylacrylic acid (TFAA), allylamine, 1-vinylimidazole (VI), 2- & 4-vinylpyridine, *N*,*N*-diethylamino ethyl methacrylate (DEAEM), acrylamide, 2-hydroxyethyl methacrylate (HEMA) and styrene. The cross-linking monomers modelled were selected to include range of compounds: *m*- & *p*- DVB, *mono-*, *di-*, *tri & tetra*- ethylene glycol dimethacrylate (EGDMA), trimethylolpropane trimethylacrylate (TRIM). A combination of commonly used porogens and solvents with known melamine solubility were modelled; these were dimethylformamide (DMF), acetonitrile, chloroform, ethanol, methanol, acetone, ethylene glycol, DMSO and water.

2.4 Molecular dynamics

2.4.1 Method 1

Determination of the stoichiometric ratio of template-FM was done via an established simulated annealing process, described elsewhere (16–18) using the SYBYL molecular modelling suite. A virtual cubic box containing one template molecule is packed with monomers until saturation capacity. The box is then reduced to its minimal dimensions to guard against excessive expansion of the mass as a result of repulsion between the molecules during the simulation. This box is then heated to 600ºK and temperature reduced in four 25 femtosecond steps to 300ºK during which time the molecules will have initially high and then decreasing mobility, allowing them to relax and orientate themselves into the position of lowest energy and thus forming a complex with the template molecule. Once the simulation is complete, the stoichiometric ratio is determined by the number of monomers bonded to the template molecule.

2.4.2 Method 2

The structures of melamine and itaconic acid molecules were downloaded from ZINC database (19) and then minimized using tools from the Chimera program (20). The melamine molecule was placed in box (3.6×3.6×3.0 nm) with itaconic acid monomers. The resulting system consisted of ca. 2175 atoms. The AMBER99sb force field was applied (21). Parameters for itaconic acid and melamine molecules were derived using the ACPYPE program using default parameters (22). The system was energy minimised and then two cycles of geometry optimisation (GO) were applied using GROMACS 4.5.5 (13). The first GO was carried out at 300 K and 1 atm by performing 1 ns of gradual annealing, thus the temperature was gradually increased from 0 to 300 K. The second GO simulation was realised at 300 K and 1 atm by performing 200 ps. The system was geometry optimised in two cycles comprising 800 steps of steepest descent followed by 3,000 steps of

conjugate gradient. During the GO phases, Berendsen thermostat and barostat (23) were applied to control the temperature and pressure, respectively. The LINCS algorithm (24) as used to constrain all bond lengths involving hydrogen atoms and an integration time step of 2 fs was used. Periodic boundary conditions (PBC) were applied. Long-range electrostatic interactions were treated using the particle mesh Ewald (PME) method (25). The cut-off radius for the real part of the electrostatic interactions, as well as for the van der Waals interactions was set to 1 nm. At the end of these GOs, the number of hydrogen bond interactions between melamine and itaconic acid molecules was extracted by using Chimera software.

2.5 Preparation of polymers and MIPs

The protocol for the synthesis of the MIP and control polymer was calculated with the aid of the MIP database's polymer calculator (http://mipdatabase.com/calc/calc.php). Using this calculator, speedy and accurate conversion of the determined molar ratios to usable masses and volumes, were calculated using the built-in compound parameters, accessible from drop down menus.

Following the solubility trials for melamine which determined DMSO as porogenic solvent of choice with the most favourable solubility, miscibility trials were conducted to compare DMSO with other (more compatible) solvents. 4 mL of chloroform, MeCN and DMSO were mixed with an equal volume of DVB and 44 mg of AIBN initiator in glass vials. The solutions were then agitated, degassed, sealed and polymerised at 60ºC for 24 hours.

For the preparation of the MIP, 1 mmol of melamine was combined with 8 mmol of itaconic acid in 4 mL (4.4 g) of DMSO in a 20 mL screw-topped glass vial. The mixture was then sonicated until all solids were dissolved. 24.8 mmol of DVB was then added and mixed to homogeneity followed by 44 mg, 0.268 mmol of the initiator was added. This was AICN for UV and 80°C polymerisations and AIBN for the 60°C polymerisation. The mixture was purged with nitrogen for 5 minutes

following thorough mechanical mixing. The vial was then sealed. Control polymers were synthesised in an identical process with the omission of the melamine template.

Thermally mediated polymerisations were carried out in an oil bath for 24 hours. For UV mediated polymerisations, the vials were instead placed into a UV reactor using a Hönle 100 UV lamp (intensity 0.157 W/cm²) (Hönle UV, UK) until turbidity was observed at which point these vials were transferred to an 80°C oil bath for 24 hours. Following polymerisation, all vials were removed and broken. Then the polymer was collected, ground and sieved to extract the 25 to 106 μm fraction which was washed with methanol for 24 hours in a Soxhlet (30 minutes approx. per cycle) and dried at 70°C until a stable weight was observed.

2.6 SEM analysis

SEM analysis was executed using a MERLIN FE-SEM (Zeiss GmbH, Jena, Germany).

2.7 N_2 Pore size analysis

Pore size and surface area analyses were carried out using a NOVA 1000 E Series Gas Sorption Analyser (Quantachrome Instruments, FL, USA) and interpreted using nitrogen BET theory (26) via the NovaWin software software package.

2.8 Column packing and HPLC calculations

The HPLC columns used were stainless steel (50 mm× 4.6 mm) into which the polymer was packed using Slurry Packer model 1666 (Alltech, UK). This process entailed mixing the polymer particles in methanol and packing the column to a pressure of 100 bar. The columns were then tightly closed and washed with the mobile phase until a steady baseline was observed.

All HPLC experiments were conducted using a Agilent 1100 HPLC and recorded using Chemstation package (Agilent, CA, USA) and performed in triplicate (n=3). Polymer characterisation was executed using a mobile phase consisting of 50:50:0.05 water: MeCN: formic acid.

UV detectors were set to wavelengths of 204 and 240 nm. The dead volume, t_0, of the column was determined by the retention time of an injection of the mobile phase containing 10% acetone. Recovery fraction was calculated as the area under the curve of the peak relative to the area under the curve created by the analyte when injected without a column present given by equation 1.

$$Recovery\% = \frac{Revoveredconcentration}{Injectedconcentration} \times \frac{100}{1} \quad (1)$$

The retention factor 'k' was calculated using the formula give in equation 2.

$$k = \frac{t_r - t_0}{t_0} \quad (2)$$

Where t_r is the retention time of the analyte taken at maximum peak height and t_0 is the dead volume of the column. The separation factor 'σ' of the polymer was calculated by equation 3.

$$\sigma = \frac{k_{melamine}}{k_2} \quad (3)$$

Where the subscript denotes the k value for each respective analyte; all calculations were done relative to $k_{melamine}$. The imprint factor 'α' of the polymer was determined using equation 4.

$$\alpha = \frac{k_{MIP}}{k_{NIP}} \tag{4}$$

The theoretical plate number, representing the degree of interaction between the analyte and the polymer, was calculated by equation 5.

$$N = 5.545\left(\frac{t_r}{w_h}\right)^2 \tag{5}$$

Where t_r is the retention time of the analyte and w_h is the peak width at half height; this was normalised with respect to the length of the column by calculating the height equivalent to a theoretical plate (H) given by equation 6.

$$H = \frac{L}{N} \tag{6}$$

Where L is the length of the column.

2.9 Milk sample preparation

All milk samples were prepared identically. For powdered samples, they were mixed with water to a concentration of 1 gram in 10 mL. Samples were then mixed in falcon tubes at a ratio of 1:1 with the acetonitrile and spiked with melamine to a concentration of 10 μM and agitated for several

minutes. The solids were then separated from the liquid via centrifugation at 5000 RPM for 5 minutes. All samples were also prepared and analysed without adulteration with melamine to confirm their purity and also to establish a base line.

3. Results and discussion

3.1 Solvation of melamine into the porogen and the use of computational modelling

As the objective of this work was to produce a molecularly imprinted bulk porous polymer resin, suitable for use as a HPLC column packing media, several criteria had to be satisfied. The first and foremost of these is to find a combination of template, FM and solvent which may facilitate the formation of template-FM complexes which could then be physically secured in place via subsequent polymerisation of a co-monomer. Computer modelling offers an accurate way to accelerate the selection process by creating a short list of candidates from larger libraries which may then be tested in the laboratory. In bulk imprinting, the template must be dissolved in the porogen at a concentration somewhere in the range of 0.25 – 0.4 $mol \cdot L^{-1}$. This concentration ensures a high number of binding sites while still ensuring a high percentage of cross-linking polymer to maintain structural rigidity. However, the high template concentrations typically present in the MIP solution can also significantly affect its thermodynamic stability and cause significant differences in all families of pore morphology relative to the NIP control (Figure 1).

Figure

Ahead of laboratory tests, melamine was screened against virtual libraries of common FMs, cross-linkers and solvents. This was done primarily due to the exceptionally poor solubility of the molecule in the conventionally used porogenic solvents. A search of the literature for melamine non-covalent imprinting protocols showed the most commonly used solvating porogen was pure

methyl alcohol (27,28), a mixture of water and methyl or ethyl alcohol (29–31), or a dispersion of chloroform in water (32). Two further works reported the successful detection of melamine using cyromazine, a structural analogue of melamine, as a template and water-alcohol binary porogenic solvent (33,34). One additional work also reported the successful use of benzene (35) as the porogen. All these cited works used the methacrylate monomers MAA and EGDMA and relied on strong solvent interactions in addition to the enhancement of template solubility provided by the FM. While it is clear that such attempts have yielded favourable results, the apparent necessity to employ solvents of high polarity and hydrogen-bonding capacity must be assumed to be a significant source of disruption to the formation of high affinity template-FM complexes in the solution (36,37).

An alternative to this approach is the use of ethylene glycol as a porogen in order to dissolve the melamine (38). While melamine has comparatively high solubility in ethylene glycol, it also has extremely high hydrogen bonding capacity and viscosity making it a challenging candidate for use as a porogenic solvent (36). The solution employed by Yusof et al. was to use an imprinting mechanism based on aromatic and Van der Waals interactions between melamine and 9-vinylcarbazole. Mechanical mixing was used to facilitate radical mobility within the solution and to reduce autoacceleration.

3.1.1 Computational modelling and laboratory trials

Since the existing protocols did not satisfy the requirements of this work, methodical laboratory pre-polymerisation trials were conducted to find an optimal combination of FM and solvent which would facilitate the solvation of melamine at a sufficient concentration and ultimately produce an effective MIP. The *ab initio* use of virtual screening models in concert with laboratory trials to confirm these predictions ahead of any polymerisation event allows for the negation of any intermolecular differences in monomer reactivity which might otherwise affect the apparent results

if the affinity of the FM candidates were compared in their polymerised form. Computationally determined affinity rankings were used to create a logical order of candidates. A summary of these results can be seen Figure 2.

Figure

Though the virtual scoring algorithm employed (described in detail elsewhere (39)), is optimised to predict the probability of hydrogen bond formation and strength, it cannot predict to what degree the intermolecular affinity and the formed complex will affect or augment the individual solubilities of each of the two molecules when combined in a solvent. Due to the poor solubility of melamine in organic solvents, the enhancing effect of the FM was heavily relied on its ability to dissolve it. Melamine's three amine groups, causing it to have a weakly basic nature, are most disposed to complex with acidic functional groups with respect to the enhancement of its solubility. Monomers HEMA and acrylamide were unable to dissolve melamine in any solvent to the degree where conventional methods of molecular imprinting would be feasible.

Having failed to dissolve melamine in several conventional porogenic solvents, it was observed that each of the three acidic FMs, shown in Figure 2, could enhance the solubility of the template in DMSO to a level of 0.25 mol·L or 1 mmol in 4 mL. This implies e.g. an increase of template solubility by one order of magnitude for melamine, caused by the addition of the IA (40). DMSO, though less commonly used than porogens such as DMF, acetonitrile or chloroform due to its relatively high polarity in addition to its augmented hydrogen bonding capacity and Hansen solubility parameters (δ_T) (36,37) may be acceptable where the template-FM complex is sufficiently durable. This is also reflected in the similar melamine-affinity scores given to both of these solvents by the molecular model (Figure 2).

3.1.2 Selection of the cross linking monomer

For bulk synthesised MIPs, the addition of the cross-linking monomer can significantly alter the equilibrium of the solution. This equilibrium shift is especially apparent when the template molecule is present at saturated levels or if the complex between the FM and template is weak. Such a change in solution parameters can lead to the precipitation of the template in solution through the breakage of the stabilising bonds within the dissolved complex. While the use of a cross-linking monomer with higher template affinity may guard against this precipitation of low solubility templates, the consequence of this may be a higher incidence of non-specific interactions during post-polymerisation testing and use of the MIP.

Di-, *Tri-*, and *Tetra-* EGDMA exhibit increasing hydrophilic character. These monomers can be used as cross-linkers when a low solubility template or an unstable template-FM complex is being imprinted (41,42). The presence of an increasing number of oxygen atoms might also augment the probability of non-specific binding since they can each be employed as acceptor atoms in the formation of a hydrogen bond (43). This can lead to lower specificity and poor imprint factors (IF). Conversely it is preferred to use cross-linking monomers which exhibit low affinity towards the template and thus does not compete with the binding mechanism of the template-FM complex. One combination of such a MIP is the use of MAA and DVB as FM and cross-linker respectively (44) whereby the weaker van der Waals interactions between a template and cross-linker do not interfere with stronger hydrogen-bonds formed by the template and FM at the receptor site.

One of the most commonly used FMs, MAA, was rejected for this work because its predicted affinity was deemed too similar to that of the porogen DMSO. This has been confirmed by poor stability of melamine in a corresponding monomer mixture containing MAA. This precipitation did not occur when the higher affinity cross-linkers, EGDMA or DEGDMA, were added. These

methacrylate monomers were also rejected as the affinity of these cross-linkers to melamine was interfering with the melamine-FM complex.

Ultimately, the combination of melamine, IA, DVB and DMSO for template, FM, cross-linker and porogen respectively, was considered to be optimal. The strength of the melamine-IA complex could also be immediately observed due to the stability of the solution upon the addition of the low affinity cross-linker DVB to monomer mixture, where no precipitation was observed.

Though IA and DVB was seen to be an excellent combination for the formation of a highly selective MIP, the necessity to use DMSO as a porogen in order to dissolve melamine raised concerns about the dynamic miscibility of the solution during polymerisation. Though the difference in δ_T is an initially negligible issue due to the relatively low molecular weights of the (*mono*) DVB and DMSO, it becomes a hindrance to the homogeneous dispersion of DVB throughout the DMSO during polymerisation as the chain length and augmented molecular weight finally induces phase separation (45). To confirm the feasibility of the use of DMSO as a porogen in this scenario, DVB polymer blanks were prepared using DMSO as well as the more commonly used porogens, chloroform and acetonitrile. SEM micrographs were taken to view the effect of the porogen on the formation of the second and third family pore structures with respect to increasing δ_T (46).

As can be seen in Figure 3, the pore structure of the chloroform-DVB polymer shows high homogeneity with all microspheres completely merged. The intermediate δ_T of the acetonitrile-DVB combination yielded adequate third family pore formation albeit with the merged microsphere-aggregates clearly visible in the morphology. Apparent puckering in the surface of the DMSO-DVB shows the endurance of the early stage microsphere-morphology due to a more abrupt phase transition. However, an acceptable third family pore structure is visible to a degree comparable to

that of the acetonitrile-DVB polymer and was thus deemed satisfactory for use as a porogen for the DVB polymer.

Figure

3.2 Thermodynamic calculation of stoichiometric ratio and MIP composition

As an improvement on the standard 1:4 ratio generally employed in laboratory syntheses (47), determination of the ideal stoichiometry of a potential template-FM combination can allow for a greater deal of insight during the polymer and protocol design process. In order to optimise MIP composition, the knowledge of the ideal stoichiometric ratio between the template and FM, melamine and IA was required. By calculating the maximum number of FM molecules capable of forming high quality hydrogen bonds with the template, specificity and sensitivity can be maximised. This was achieved through minimisation of the formation of lower affinity binding sites (48).

The use of a computationally determined ratio alone, which is calculated under ideal conditions, has been reported to produce an inferior MIP with a high incidence of non-specific and heterogeneous binding behaviour caused by the disruption of the majority of the template-FM complexes by the solvent and cross-linker (49). For this reason, an excess of monomer as a 'factor of safety' was added to the calculated ideal ratio. This factor of safety cannot be an unchecked saturation of the solution with the FM as this can also lead to FM-aggregation or dimerisation, also leading to a net reduction of receptors within the MIP (15,47,50).

Melamine-IA stoichiometric ratios of 6 were calculated by both computational methods attempted with both complexes showing identical bonds for each (Figure 4). This ratio of 6 with respect to the

use of a carboxylic dipole is also independently confirmed by a third method recently published in the literature (28). This ideal ratio of 6 was increased to 8 for the practical synthesis of the MIP.

Figure

Thus the newly determined parameters for molecular dynamics protocol utilising the Gromacs open source molecular dynamics package were doubly confirmed. This confirmation of the Gromacs protocol is of added interest due to its departure from convention of the relaxation of the FM around the template via simulated annealing, from elevated to ambient temperature which has been the method of choice for the calculation of template-FM stoichiometric ratio to date. The Gromacs process, conversely, relies on a series of minimisation cycles and a relaxation phase in the form of a gradual annealing followed by a relaxation step at 300 K. This strategy allows the calculation to be applied to thermally sensitive or biological molecules and, in this particular case, enables the geometric optimization of the monomers around the template (51,52).

Having determined the optimal volumes of melamine, IA and DMSO which were dictated by stoichiometry and solubility limits, the calculation of the exact volume of cross-linker and initiator was calculated with the aid of the free online polymer calculator from the MIP database (see Materials and Methods). This allows for the facile calculation of all molecular and volumetric ratios with the inbuilt unit conversion facility. In this way, the masses or volumes of all of the polymerisation mixture can be balanced against the required volume of porogenic solvent, typically constituting to 50% of the total solution (47).

3.3 Selection of initiator and polymerisation temperature

The rate of radical propagation, of chain growth and the thermodynamic 'goodness' of the solvent all affect the point at which chain collapse and precipitation into the solution occurs. This

precipitation point can be significantly delayed or advanced depending on the effect of the template. When the template has a high level of solubility in the porogen, the thermodynamic stabilisation of oligomer during chain growth leads to an enhancement in pore and precipitate size (3). Alternatively, as is the case in this study, the decreased stability that melamine imbues to the growing oligomer was seen to force the precipitation of the chain at a shorter molecular weight and thus reduce the pore structure and net surface area of the polymer. Adding to the complexity of this effect is the enhancement of melamine solubility in DMSO with respect to increased temperature (53) which increases the stability of solvated melamine-IA complexes though any increase in temperature will have a similar effect on the rate of radical propagation (54). A general rule of MIP synthesis with respect to the formation of selective binding sites is that the process should take place over a long period of time, at a low temperature and with a low concentration of initiator (55). However, as is the present case, the final application of HPLC column packing media and the low thermodynamic stability of the melamine-IA complex required an elevated temperature to maintain sufficient mechanical rigidity and oligomer stability. The mass of the initiator was, however placed at a constant value of 44mg or 1% of the total monomer mass.

Two radical initiators were selected for polymerisation both of which had differing rates of decomposition (k_d) with AIBN at 60ºC and AICN at 80ºC decomposing at rates of approximately $17x10^{-5}$ s^{-1} and $6.5x10^{-6}$ s^{-1} respectively (49). The latter can also be initiated via UV excitation at room temperature. The destabilising effect of melamine on the polymerisation process was most evident during room temperature polymerisation whereby phase separation was occurring 33% faster than in the case of the control. This clear and immediate demonstration of oligomer destabilisation in solution by melamine was reflected when the results of the porosity and surface area measurements were analysed (Table 1). Pore volume was reduced by one order of magnitude due to this effect with a similar reduction in total surface area. Due to the increased rate of radical propagation resulting from the AIBN-initiated polymerisation at 60ºC, the pore volume was notably

reduced from that of the slower radical production rate of the AICN-initiated polymerisation at 80ºC. The pore volume of the NIP control was 140% that of the MIP. While the difference in surface area between the MIPs and NIPs of the two thermally initiated polymers was comparable, the very similar pore volume of the AIBN-initiated MIP and NIP cause it to be ultimately selected for further tests as it allowed for the most accurate analysis of the imprint factor.

Table

3.4 Mobile phase selection and polymer characterisation

Following its selection as the polymer most comparable to its control, the AIBN-initiated MIP, polymerised at 60ºC, was packed into HPLC columns. The use of the MIP as the stationary phase in a HPLC flow system has the distinct advantage of reducing the required detection time by decreasing the number of preparatory steps and negating the need for a separate regeneration process, as is the case with the more commonly used SPE method of detection. As a goal of this work was to create such an incorporated sensor, a comprehensive characterisation of the MIP was carried out under conditions typical to the detection of melamine-contaminated milk (56). To facilitate the MIP's accurate characterisation, acidification of the mobile phase was necessary due to the failure of FM-FM dimerisation events during polymerisation. This dimerisation of surplus functional groups is essential to minimise non-specific interactions between the polymer and target, the absence of which may lead to the complete negation of any apparent imprinting event via the higher incidence of exposed functional groups at the surface of the polymer (47). This phenomenon was made apparent by a high retention time, notably greater than that of the MIP, exhibited by the NIP toward melamine when a purely aqueous mobile phase was tested. This high retention time was accompanied by broad peak with extreme tailing caused by the exposure of IA-carboxylic groups on the surface of the NIP. Interestingly, in addition to the reduced retention time, the MIP column also showed a greatly reduced level of tailing which was attributed to the higher level of order and

reduced accessibility of the functional groups as more were engaged in a single receptor site at the MIP surface. The non-specific interactions exhibited by the NIP were disrupted with the acidification of the mobile phase with a weak acid. With the addition of 0.05% formic acid, the imprinting factor could be viewed and the polymer specificity characterised.

It was immediately notable that the peak tailing was still present in the NIP control even when the optimised mobile phase was implemented (Figure 5). Tailing was far less of an issue in the case of the MIP and its narrower peaks were accompanied with increased peak-symmetry. Optimisation of experimental conditions showed an increase in imprinting factor (α) with respect to reduced concentration and flow rate with a maximum value of 2.25 (Figure 6). A flow rate of 0.5 $mL \cdot min^{-1}$ was ultimately selected due to practicality of the analysis.

Figure

Figure

Cross-response of the polymer under these conditions could then be analysed. It was seen that due to the low affinity of the cross-linking polymer, DVB, specificity towards melamine could be rapidly achieved while secondary molecules were flushed trough the column without any interaction (Table 2). Acetoguanamine, the molecule which exhibited a retention factor (k) most similar to melamine, is retained notably longer on the non-imprinted polymer than melamine due to a higher primary affinity towards IA. This order is reversed on the MIP and must be attributed to the morphology of the imprinted receptors within its structure. Melamine recovery is also superior in the case of the MIP while for all other secondary molecules tested; the NIP control displayed improved recovery for all other secondary molecules tested.

Table

3.5 Testing on spiked real milk samples

Having confirmed the efficacy of the imprinting protocol and the resulting polymer, milk samples were prepared to test the ability of the MIP to detect melamine in its known role as an adulterant in dairy products. Five samples were selected from local supermarkets in order to encompass a range of fat contents and product lifespans (Table 3). It was in the screening of these spiked samples that the limitation of the combined effect of the column length and polymer surface area was made apparent. The efficiency of separation power of MIP (as well as the Blank) columns did not allow separation of the melamine peak from all other compounds in all five samples tested (Table 2). For this reason, the organic fraction of the mobile phase was increased by 50% to improve peak separation. This had the desired effect and good recovery could be observed in four of the five samples tested (Table 4). The powdered samples showed greater levels of absorbance overall, possibly due to the presence of nondescript fibre within them, stated as being present at levels of 0.1% in sample 5. Improved recovery percentages using this polymer may be achieved with the use of a longer column which would compensate somewhat for the lower surface area observed in the MIP resulting from melamine's solubility issues.

Table

Table

3.6 Comparison with the literature

When attempting to imprint a low solubility molecule such as melamine, several strategic choices and compromises must be made in order to satisfy the objectives of a given project and thus procure certain advantages and disadvantages. In this work, this has been the production of a rapid and

specific, single step method for the detection of melamine in real samples. A brief summary of the properties of the MIP detailed in this current work is compared with those reported in the literature can be seen in Table 5.

Table

4. Conclusions

A new MIP HPLC column for the detection of melamine in milk has been described. Using virtual screening methods, laboratory screening time was greatly reduced. Solvent-polymer compatibility, template affinity and polymerisation conditions were confirmed through virtual and practical methods to produce an optimised imprinted polymer. A novel new protocol was presented for the determination of template-FM stoichiometric ratio using the open source molecular dynamics software suite, Gromacs. The minimisation of affinity between cross-linking polymer and melamine, the target, allowed for a rapid and selective analysis process which, under optimised conditions took 7 to 8 minutes. The maximum imprinting factor of the polymer column was calculated to be 2.25 and showed discriminative preference for melamine at concentrations from 100 to 1 μM. This MIP-HPLC based analysis system is a promising tool for the detection of melamine in food products.

5. Acknowledgements

This research was supported by the Research Executive Agency (REA) of the European Union under Grant Agreement number PITN-GA-2010-264772 (ITN CHEBANA) and the Spanish ministry of economy MINECO (Project CTQ2013-41577-P). M. del Valle acknowledges support by the Catalonia program ICREA Academia.

6. References

1. Haupt K, Mosbach K. Molecularly Imprinted Polymers and Their Use in Biomimetic Sensors.

Chem Rev. 2000 Jul 1;100(7):2495–2504.

2. Whitcombe MJ, Kirsch N, Nicholls IA. Molecular imprinting science and technology: a survey of the literature for the years 2004-2011. J Mol Recognit. 2014 Jun;27(6):297–401.
3. Bates F, del Valle M. Voltammetric sensor for theophylline using sol–gel immobilized molecularly imprinted polymer particles. Microchim Acta. 2015 Apr;182(5–6):933–942.
4. Rovina K, Siddiquee S. A review of recent advances in melamine detection techniques. J Food Compos Anal. 2015 Nov;43:25–38.
5. National Toxicology Program. NTP Carcinogenesis Bioassay of Melamine (CAS No. 108-78-1) in F344/N Rats and B6C3F1 Mice (Feed Study). Natl Toxicol Program Tech Rep Ser. 1983 Mar;245:1–171.
6. Ogasawara H, Imaida K, Ishiwata H, Toyoda K, Kawanishi T, Uneyama C, et al. Urinary bladder carcinogenesis induced by melamine in F344 male rats: correlation between carcinogenicity and urolith formation. Carcinogenesis. 1995 Nov;16(11):2773–2777.
7. Panuwet P, Wade EL, Nguyen JV, Montesano MA, Needham LL, Barr DB. Quantification of cyanuric acid residue in human urine using high performance liquid chromatography–tandem mass spectrometry. J Chromatogr B. 2010 Oct 15;878(28):2916–2922.
8. Skinner CG, Thomas JD, Osterloh JD. Melamine toxicity. J Med Toxicol. 2010 Mar;6(1):50–55.
9. Lynch JM, Barbano DM. Kjeldahl nitrogen analysis as a reference method for protein determination in dairy products. J AOAC Int. 1999 Dec;82(6):1389–1398.
10. Venkatasami G, Sowa JR. A rapid, acetonitrile-free, HPLC method for determination of melamine in infant formula. Anal Chim Acta. 2010 Apr 30;665(2):227–230.
11. Gossner CM-E, Schlundt J, Ben Embarek P, Hird S, Lo-Fo-Wong D, Beltran JJO, et al. The Melamine Incident: Implications for International Food and Feed Safety. Environ Health Perspect. 2009 Aug 6;117(12):1803–1808.
12. Li Y, Xu J, Sun C. Chemical sensors and biosensors for the detection of melamine. RSC Adv.

2015;5(2):1125–1147.

13. Pronk S, Pall S, Schulz R, Larsson P, Bjelkmar P, Apostolov R, et al. GROMACS 4.5: a high-throughput and highly parallel open source molecular simulation toolkit. Bioinformatics. 2013 Apr 1;29(7):845–854.
14. Chianella I, Lotierzo M, Piletsky SA, Tothill IE, Chen B, Karim K, et al. Rational Design of a Polymer Specific for Microcystin-LR Using a Computational Approach. Anal Chem. 2002 Mar;74(6):1288–1293.
15. Piletsky SA, Karim K, Piletska EV, Turner APF, Day CJ, Freebairn KW, et al. Recognition of ephedrine enantiomers by molecularly imprinted polymers designed using a computational approach. The Analyst. 2001;126(10):1826–1830.
16. Subrahmanyam S, Piletsky SA, Piletska EV, Chen B, Karim K, Turner AP. "Bite-and-Switch" approach using computationally designed molecularly imprinted polymers for sensing of creatinine11Editors Selection. Biosens Bioelectron. 2001 Dec;16(9–12):631–637.
17. Piletsky S, Piletska E, Karim K, Foster G, Legge C, Turner A. Custom synthesis of molecular imprinted polymers for biotechnological application. Anal Chim Acta. 2004 Feb;504(1):123–130.
18. Lakshmi D, Akbulut M, Ivanova-Mitseva PK, Whitcombe MJ, Piletska EV, Karim K, et al. Computational Design and Preparation of MIPs for Atrazine Recognition on a Conjugated Polymer-Coated Microtiter Plate. Ind Eng Chem Res. 2013 Oct 2;52(39):13910–13916.
19. Irwin JJ, Sterling T, Mysinger MM, Bolstad ES, Coleman RG. ZINC: A Free Tool to Discover Chemistry for Biology. J Chem Inf Model. 2012 Jul 23;52(7):1757–1768.
20. Pettersen EF, Goddard TD, Huang CC, Couch GS, Greenblatt DM, Meng EC, et al. UCSF Chimera--A visualization system for exploratory research and analysis. J Comput Chem. 2004 Oct;25(13):1605–1612.
21. Hornak V, Abel R, Okur A, Strockbine B, Roitberg A, Simmerling C. Comparison of multiple Amber force fields and development of improved protein backbone parameters. Proteins Struct

Funct Bioinforma. 2006 Nov 15;65(3):712–725.

22. Sousa da Silva AW, Vranken WF. ACPYPE - AnteChamber PYthon Parser interfacE. BMC Res Notes. 2012;5(1):367.
23. Berendsen HJC, Postma JPM, van Gunsteren WF, DiNola A, Haak JR. Molecular dynamics with coupling to an external bath. J Chem Phys. 1984;81(8):3684.
24. Hess B, Bekker H, Berendsen HJC, Fraaije JGEM. LINCS: A linear constraint solver for molecular simulations. J Comput Chem. 1997 Sep;18(12):1463–1472.
25. York DM, Wlodawer A, Pedersen LG, Darden TA. Atomic-level accuracy in simulations of large protein crystals. PNAS. 1994;91(18):8715–8718.
26. McMillan WG, Teller E. The Assumptions of the B.E.T. Theory. J Phys Chem. 1951 Jan;55(1):17–20.
27. Zhu L, Xu G, Wei F, Yang J, Hu Q. Determination of melamine in powdered milk by molecularly imprinted stir bar sorptive extraction coupled with HPLC. J Colloid Interface Sci. 2015 Sep 15;454:8–13.
28. Wang Y, Liu J-B, Tang S-S, Jin R-F. Preparation of melamine molecularly imprinted polymer by computer-aided design. J Sep Sci. 2015 Aug;38(15):2647–2654.
29. Yang H-H, Zhou W-H, Guo X-C, Chen F-R, Zhao H-Q, Lin L-M, et al. Molecularly imprinted polymer as SPE sorbent for selective extraction of melamine in dairy products. Talanta. 2009 Dec 15;80(2):821–825.
30. He D, Zhang X, Gao B, Wang L, Zhao Q, Chen H, et al. Preparation of magnetic molecularly imprinted polymer for the extraction of melamine from milk followed by liquid chromatography-tandem mass spectrometry. Food Control. 2014 Feb;36(1):36–41.
31. Lian Z, Liang Z, Wang J. Determination of melamine in aquaculture feed samples based on molecularly imprinted solid-phase extraction: Other Techniques. J Sep Sci. 2015 Oct;38(20):3655–3660.
32. Figueiredo L, Santos L, Alves A. Synthesis of a Molecularly Imprinted Polymer for Melamine

Analysis in Milk by HPLC with Diode Array Detection. Adv Polym Technol. 2015 Dec;34(4)

33. He L, Su Y, Shen X, Zheng Y, Guo H, Zeng Z. Solid-phase extraction of melamine from aqueous samples using water-compatible molecularly imprinted polymers. J Sep Sci. 2009 Oct;32(19):3310–3318.
34. Yan H, Cheng X, Sun N, Cai T, Wu R, Han K. Rapid and selective screening of melamine in bovine milk using molecularly imprinted matrix solid-phase dispersion coupled with liquid chromatography-ultraviolet detection. J Chromatogr B. 2012 Nov 1;908:137–142.
35. Liang R, Zhang R, Qin W. Potentiometric sensor based on molecularly imprinted polymer for determination of melamine in milk. Sens Actuators B Chem. 2009 Sep;141(2):544–550.
36. Barton AFM. CRC handbook of solubility parameters and other cohesion parameters. 2nd ed. Boca Raton: CRC Press; 1991. 739
37. Reichardt C, Welton T. Solvents and solvent effects in organic chemistry. 4th, updated and enl. ed. Weinheim, Germany: Wiley-VCH; 2011. 692
38. Yusof N, Rahman S, Hussein M, Ibrahim N. Preparation and Characterization of Molecularly Imprinted Polymer as SPE Sorbent for Melamine Isolation. Polymers. 2013 Oct 23;5(4):1215–1228.
39. Nicholls I, Piletsky S, Chen B, Chianella I, Turner A. Thermodynamic Considerations and the Use of Molecular Modeling as a Tool for Predicting MIP Performance. In: Yan M, Ramström O, editors. Molecularly Imprinted Materials. CRC Press; 2004. p. 363–393.
40. Keith LH, Walters DB, National Toxicology Program (U.S.), editors. National Toxicology Program's chemical solubility compendium. Boca Raton: Lewis Publishers; 1992. 437
41. Zheng M-M, Gong R, Zhao X, Feng Y-Q. Selective sample pretreatment by molecularly imprinted polymer monolith for the analysis of fluoroquinolones from milk samples. J Chromatogr A. 2010 Apr;1217(14):2075–2081.
42. Gryshchenko A, Bottaro C. Development of Molecularly Imprinted Polymer in Porous Film Format for Binding of Phenol and Alkylphenols from Water. Int J Mol Sci. 2014 Jan

20;15(1):1338–1357.

43. Jeffrey GA. An introduction to hydrogen bonding. New York: Oxford University Press; 1997. 303 . (Topics in physical chemistry).
44. Villamena FA, De La Cruz AA. Caffeine selectivity of divinylbenzene crosslinked polymers in aqueous media. J Appl Polym Sci. 2001 Oct 3;82(1):195–205.
45. Hansen CM. Hansen solubility parameters: a user's handbook. 2nd ed. Boca Raton: CRC Press; 2007. 519.
46. Spivak D. Optimization, evaluation, and characterization of molecularly imprinted polymers. Adv Drug Deliv Rev. 2005 Dec 6;57(12):1779–1794.
47. Li J, Wei G, Zhang Y. Molecularly imprinted polymers as recognition elements in sensors. In: Li S, Ge Y, Piletsky SA, Lunec J, editors. Molecularly imprinted sensors: overview and applications. 1st ed. Amsterdam ; Boston: Elsevier; 2012. p. 35–56.
48. Castell OK, Barrow DA, Kamarudin AR, Allender CJ. Current practices for describing the performance of molecularly imprinted polymers can be misleading and may be hampering the development of the field. J Mol Recognit. 2011 Nov;24(6):1115–1122.
49. Schauperl M, Lewis DW. Probing the Structural and Binding Mechanism Heterogeneity of Molecularly Imprinted Polymers. J Phys Chem B. 2015 Jan 15;119(2):563–571.
50. Farrington K, Magner E, Regan F. Predicting the performance of molecularly imprinted polymers: Selective extraction of caffeine by molecularly imprinted solid phase extraction. Anal Chim Acta. 2006 Apr;566(1):60–68.
51. Karlsson BCG, O'Mahony J, Karlsson JG, Bengtsson H, Eriksson LA, Nicholls IA. Structure and Dynamics of Monomer−Template Complexation: An Explanation for Molecularly Imprinted Polymer Recognition Site Heterogeneity. J Am Chem Soc. 2009 Sep 23;131(37):13297–13304.
52. Dindo M, Montioli R, Busato M, Giorgetti A, Cellini B, Borri Voltattorni C. Effects of interface mutations on the dimerization of alanine glyoxylate aminotransferase and

implications in the mistargeting of the pathogenic variants F152I and I244T. Biochimie. 2016 Dec;131:137–148.

53. Ren B, Li C, Yuan X, Wang F. Determination and correlation of melamine solubility. Huagong Xuebao J Chem Ind Eng China. 2003;54(7):1001–1003.
54. Sigma Aldrich. Free radical initiators - thermal initiators [Internet]. [Accessed Sep 24 2015]. Available from: http://www.sigmaaldrich.com/content/dam/sigma-aldrich/docs/Aldrich/General_Information/thermal_initiators.pdf
55. Mijangos I, Navarro-Villoslada F, Guerreiro A, Piletska E, Chianella I, Karim K, et al. Influence of initiator and different polymerisation conditions on performance of molecularly imprinted polymers. Biosens Bioelectron. 2006 Sep;22(3):381–387.
56. Ibáñez M, Sancho JV, Hernández F. Determination of melamine in milk-based products and other food and beverage products by ion-pair liquid chromatography–tandem mass spectrometry. Anal Chim Acta. 2009 Sep;649(1):91–97.

Figure Captions

FIG 1: Schematic representation of the molecular imprinting and pore formation processes in the synthesis of a molecularly imprinted porous polymer resin

FIG 2: Histogram summarising the binding affinities of functional monomer, cross-linker monomer and solvent molecules for melamine as calculated by the SYBYL molecular modelling platform

FIG 3: SEM micrographs showing the effect of differences in δ_T and polymer-porogen miscibility on third family pore formation and homogeneity for (a) chloroform-DVB, (b) acetonitrile-DVB and (c) DMSO-DVB

FIG 4: Image of ideal melamine-IA stoichiometric complexes calculated using parameters based on (a) the SYBYL modelling platform and (b) the open source Gromacs modelling platform

FIG 5: Chromatogram of the peak corresponding to a 10 μL injection of (a) 100 μM and (b) 10 μM melamine solution in a 50:50:0.05 water, acetonitrile, formic acid and 0.5 $mL \cdot min^{-1}$ mobile phase

FIG 6: 3D histogram detailing imprint factor 'IF' as a function of flow rate and melamine concentration; injection volume was 10 μL

List of Tables

TABLE 1: Summary of porosity and surface area measurements calculated using the N_2 BET method

Polymerisation type		Radical Initiator	Polymer ID	Pore Volume ($cc \cdot g^{-1}$)	Pore radius (Å)	Surface area ($m^2 \cdot g^{-1}$)
temperature	Energy source					
20ºC	UV	AICN	MIP	0.0077	9.6	24.61
			NIP	0.0265	9.3	75.88
60ºC	Thermal	AIBN	MIP	0.1660	8.8	385.30
			NIP	0.1710	8.8	400.10
80ºC	Thermal	AICN	MIP	0.6670	8.9	432.38
			NIP	0.9483	8.9	445.10

TABLE 2: Affinity and capacity factors characterising the (a) MIP and (b) NIP for cross response at a flow rate of 0.5 mL·min^{-1} and a 10 µL injection volume of 10 µM concentration

(a)

	Retention time (min)	k	σ	α	% Recovery	N	H (mm)
melamine	4.20	1.49	N/A	1.39	94.59	43.14	1.16
acetoguanamine	4.07	1.41	1.06	0.91	78.92	29.19	1.71
Cyanuric acid	1.55	-0.08	N/A	N/A	38.45	1.09	45.71
triazine	1.74	0.03	44.38	0.05	91.99	56.48	0.89
urea	1.60	-0.05	N/A	N/A	108.25	69.30	0.72

(b)

	Retention time (min)	k	σ	% Recovery	N	H (mm)
melamine	3.29	1.09	N/A	83.3	24.61	2.03
acetoguanamine	4.02	1.55	0.70	79.14	9.78	5.11
Cyanuric acid	1.53	-0.03	N/A	56.07	0.27	187.77
triazine	2.58	0.64	1.70	100.09	6.34	7.88
urea	1.79	0.14	7.91	114.77	22.31	2.24

TABLE 3: Description and content summary (g/100 mL) of milk samples tested

Sample	Description	Fats	Carbohydrate	Protein
1	Tesco everyday value British skimmed UHT milk	1.8	4.8	3.6
2	Pensworth Full fat whole milk	3.6	4.6	3.4
3	Pensworth low fat semi-skimmed milk	1.6	4.7	3.6
4	Tesco everyday value dried milk	0.06	3.0	2.1
5	Tesco Instant dried skimmed milk with added vitamins A & D	0.05	4.6	3.3

TABLE 4: Recoveries of melamine from the 5 milk samples detailed in Table 3

Sample	% of total area	% Recovery
1	17.22	94.16
2	17.39	96.11
3	17.28	66.91
4	16.17	90.07
5	14.78	88.87

TABLE 5: List of the state of the art in comparison to this current work

Template	**Polymer format**	**Detection method**	**LOD**	**Steps**	**Measurement time**	**Ref.**
Melamine	Bulk polymerisation	Selective adsorption	0.0127 ng/mL	2	50 minutes	(27)
Melamine	Precipitated nanoparticles	Equilibrium binding	19.84 mg/g	2	12 hrs	(28)
Melamine	Bulk polymerisation	SPE	0.5μM	2	Not given	(29)
Melamine	Core-shell precipitates	Equilibrium binding	10 ng/mL	2	24 hrs	(30)
Melamine	Bulk polymerisation	SPE	0.1μg/g	2	Not given	(31)
Melamine	Suspension polymerisation	Selective adsorption	10 mg/L	2	40 minutes	(32)
Cyromazine	Bulk polymerisation	SPE	0.1 ng/mL	2	Not given	(33)
Melamine	Precipitated microparticles	SPE	53.01 mg/g	2	Not given	(38)
Melamine	Bulk polymerisation	HPLC column	1μM	1	7 minutes	This work

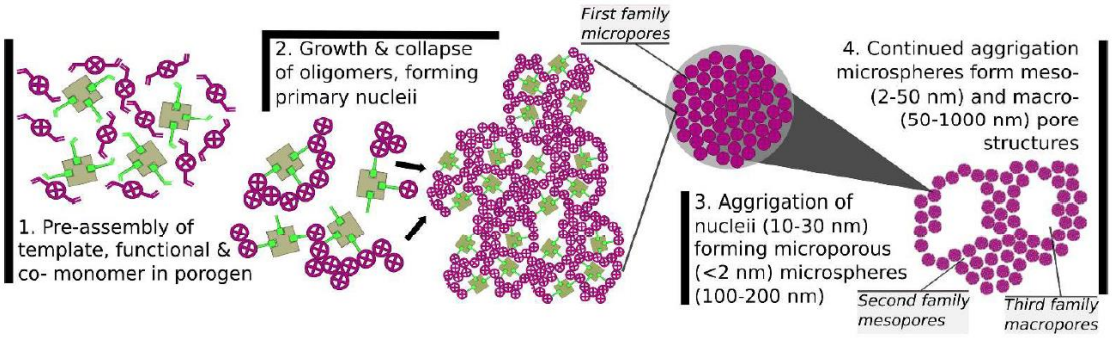
1. Pre-assembly of template, functional & co- monomer in porogen
2. Growth & collapse of oligomers, forming primary nucleii
First family micropores
3. Aggrigation of nucleii (10-30 nm) forming microporous (<2 nm) microspheres (100-200 nm)
4. Continued aggrigation microspheres form meso- (2-50 nm) and macro- (50-1000 nm) pore structures
Second family mesopores
Third family macropores

Figure 1

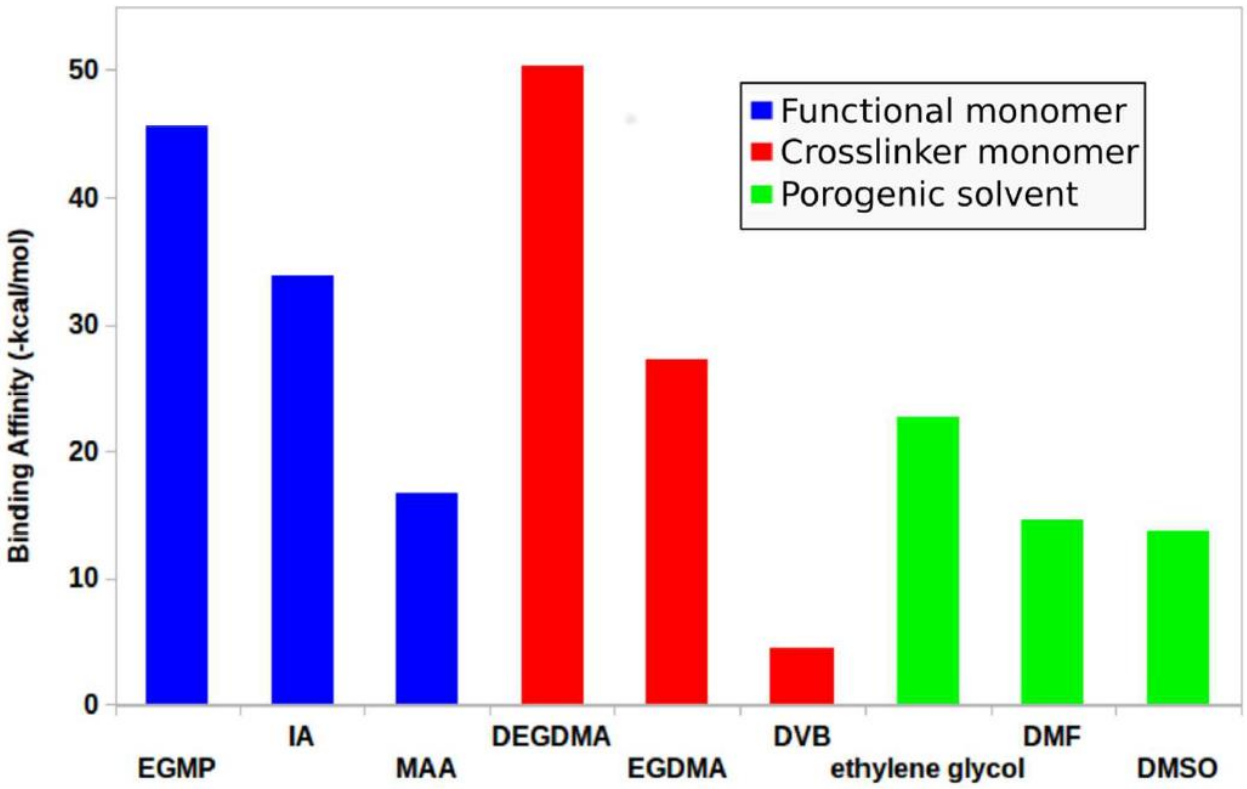
Binding Affinity (-kcal/mol)
50
40
30
20
10
0
Functional monomer
Crosslinker monomer
Porogenic solvent
EGMP
IA
MAA
DEGDMA
EGDMA
DVB
ethylene glycol
DMF
DMSO

Figure 2

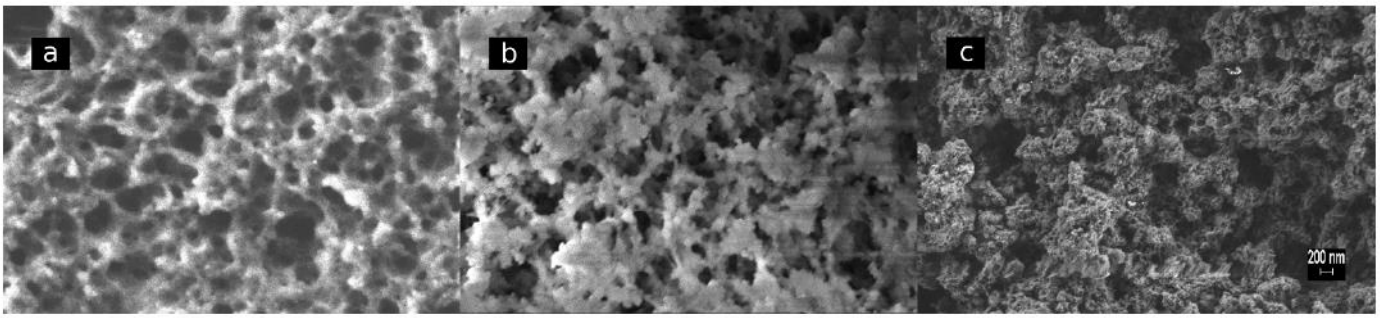

Figure 3

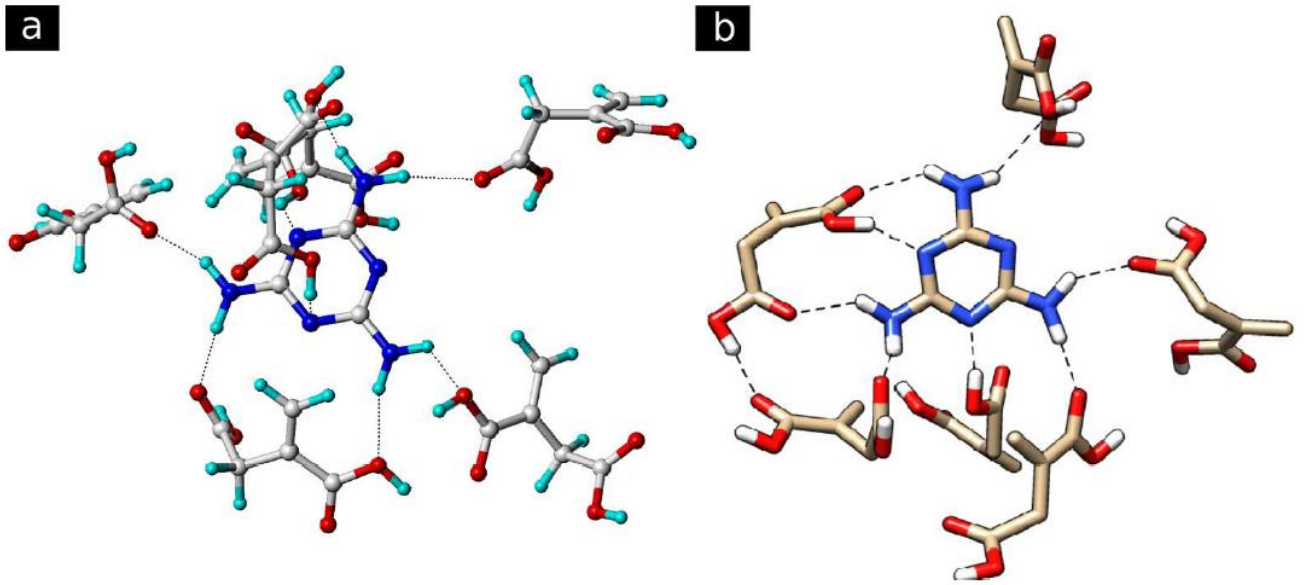

Figure 4

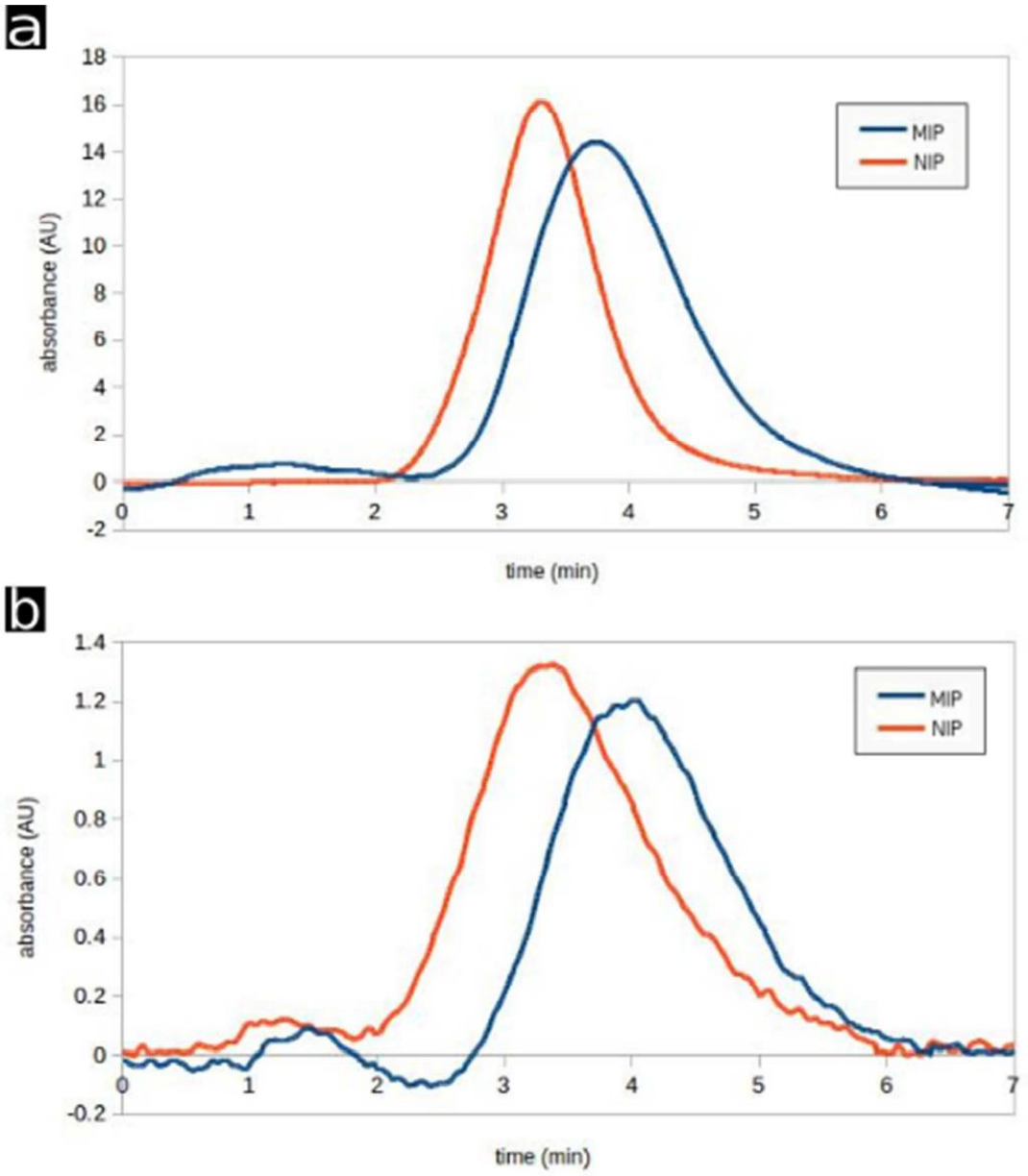
a
18
16
14
12
10
8
6
4
2
0
-2
absorbance (AU)
0
1
2
3
4
5
6
7
time (min)
MIP
NIP
b
1.4
1.2
1
0.8
0.6
0.4
0.2
0
-0.2
absorbance (AU)
0
1
2
3
4
5
6
7
time (min)
MIP
NIP

Figure 5

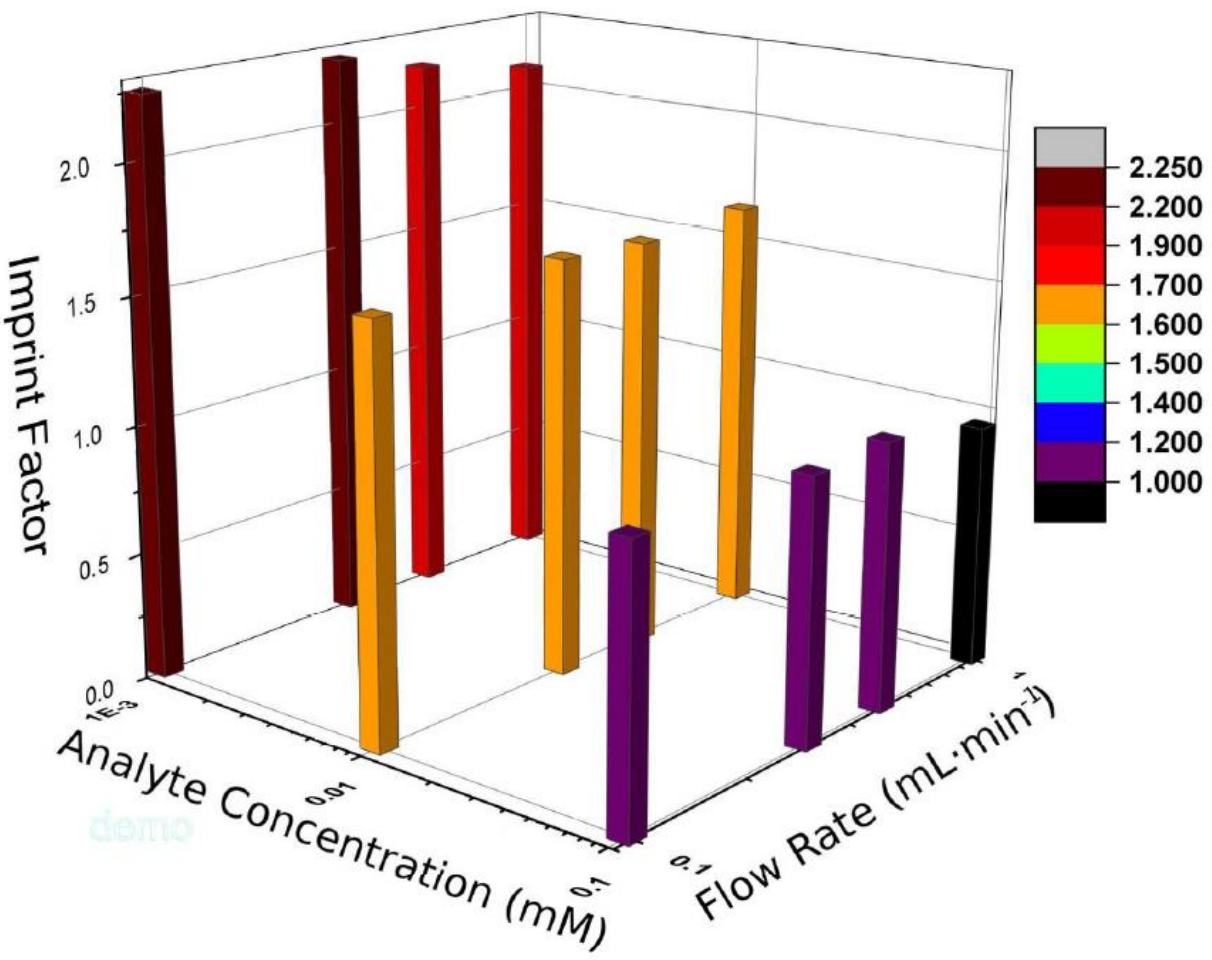
Imprint Factor
2.0
1.5
1.0
0.5
0.0
Analyte Concentration (mM)
Flow Rate (mL·min-1)
2.250
2.200
1.900
1.700
1.600
1.500
1.400
1.200
1.000

Figure 6